PALEONTOLOGY

The Emu Bay Shale: A unique early Cambrian Lagerstätte from a tectonically active basin

Robert R. Gaines[1]*, Diego C. García-Bellido[2,3], James B. Jago[3,4], Paul M. Myrow[5], John R. Paterson[6]*

The Emu Bay Shale (EBS) of South Australia is anomalous among Cambrian Lagerstätten because it captures anatomical information that is rare in Burgess Shale–type fossils, and because of its inferred nearshore setting, the nature of which has remained controversial. Intensive study, combining outcrop and borehole data with a compilation of >25,000 fossil specimens, reveals that the EBS biota inhabited a fan delta complex within a tectonically active basin. Preservation of soft-bodied organisms in this setting is unexpected and further underscores differences between the EBS and other Cambrian Lagerstätten. Environmental conditions, including oxygen fluctuations, slope instability, high suspended sediment concentrations, and episodic high-energy events, inhibited colonization of the lower prodelta by all but a few specialist species but favored downslope transportation and preservation of other largely endemic, shallow-water benthos. The EBS provides extraordinary insight into early Cambrian animal diversity from Gondwana. These results demonstrate how environmental factors determined community composition and provide a framework for understanding this unique Konservat-Lagerstätte.

INTRODUCTION

The Cambrian Explosion is marked by the sudden appearance of almost all animal phyla in the fossil record, the proliferation of predation and complex food webs, and very high rates of morphological evolution across lineages. The patterns and magnitude of this event are best understood from Konservat-Lagerstätten, deposits that include spectacular preservation of soft, nonbiomineralized tissues that offer unparalleled insight into marine biodiversity in the immediate aftermath of the Cambrian Explosion (*1*–*3*).

Among these deposits, the lower Cambrian (Series 2, Stage 4) Emu Bay Shale (EBS) of Kangaroo Island, South Australia (Fig. 1) has proven particularly important. Some EBS fossils retain anatomical aspects, such as muscle fibers (*4*) and nonbiomineralized compound eye lenses (*5*–*7*), which are rare or absent in other Cambrian Lagerstätten. The style of preservation in the EBS thus appears to be distinct from the widespread pattern of soft-tissue preservation typical of Cambrian Burgess Shale–type (BST) deposits (*8*). Critically, evaluation of the paleoecological and evolutionary significance of the EBS biota has been complicated by uncertainty surrounding its paleoenvironmental setting (*9*).

As recognized in earlier studies, the EBS accumulated in a nearshore setting (*10*), but the nature of that setting, including water depth and redox status, has remained the subject of debate (*11*–*15*). Exceptional preservation of nonbiomineralized fossils in Cambrian nearshore and shoreline sandstone deposits includes casts and molds of stranded jellyfish (*16*–*18*), casts of arthropods (*19*, *20*), and small carbonaceous fossils (*21*). The preservation of a diverse assemblage of soft-bodied macrofossils in a nearshore setting in the EBS, however, is anomalous and clearly distinct from the widespread pattern of Cambrian BST deposits. Like the EBS, BST deposits capture diverse assemblages of soft-bodied macrofossils but occur in offshore shelf and slope facies that were deposited near, but below, storm wave base (*8*, *22*).

Here, we use detailed outcrop and borehole data to interpret the paleoenvironmental setting of the EBS and, using a new dataset of >25,000 fossil specimens, establish the environmental factors that influenced the unique assemblage of the EBS biota.

RESULTS

Depositional setting of the EBS

The EBS belongs to the Kangaroo Island Group, a lower Cambrian succession that is restricted to the northeastern coast of Kangaroo Island (Fig. 1, A and B, and fig. S1). The Kangaroo Island Group has been interpreted to represent deposition near the northern (present day) boundary of an ancient rift basin with alluvial fans at its margin, and its deposition was accompanied by minor syndepositional mafic alkaline volcanism (*10*, *23*–*26*). Rifting is linked to the onset of convergent deformation associated with the Delamerian Orogeny and, more broadly, to active deformation along most of the Antarctic and Australian western margin of Gondwana (*27*).

Early workers suggested a shallow water setting for the EBS based on inferred tidal influence during deposition of adjoining units: the underlying Marsden Sandstone and overlying Boxing Bay Formation (*10*). Biomarker evidence for the presence of cyanobacteria in the EBS was used to support a shallow water setting (*12*), although transportation and burial of cyanobacterial organic matter in a deeper setting cannot be excluded. Recent geochemical study of outcrop samples using organic carbon and trace element concentrations revealed no evidence for anoxic conditions (*12*, *15*), upholding the prevailing interpretation of a well-oxygenated, shallow marine depositional setting. However, renewed field investigation led Gehling *et al.* (*11*) to suggest that the Lagerstätte-bearing interval was deposited

[1]Geology Department, Pomona College, 185 E. Sixth St., Claremont, CA 91711, USA. [2]School of Biological Sciences & Environment Institute, University of Adelaide, Adelaide, SA 5005, Australia. [3]Earth Sciences Section, South Australian Museum, North Terrace, Adelaide, SA 5000, Australia. [4]University of South Australia–STEM, Mawson Lakes, SA 5095, Australia. [5]Geology Department, Colorado College, Colorado Springs, CO 80903 USA. [6]Palaeoscience Research Centre, School of Environmental and Rural Science, University of New England, Armidale, NSW 2351, Australia.
*Corresponding author. Email: robert.gaines@pomona.edu (R.R.G.); jpater20@une.edu.au (J.R.P.)

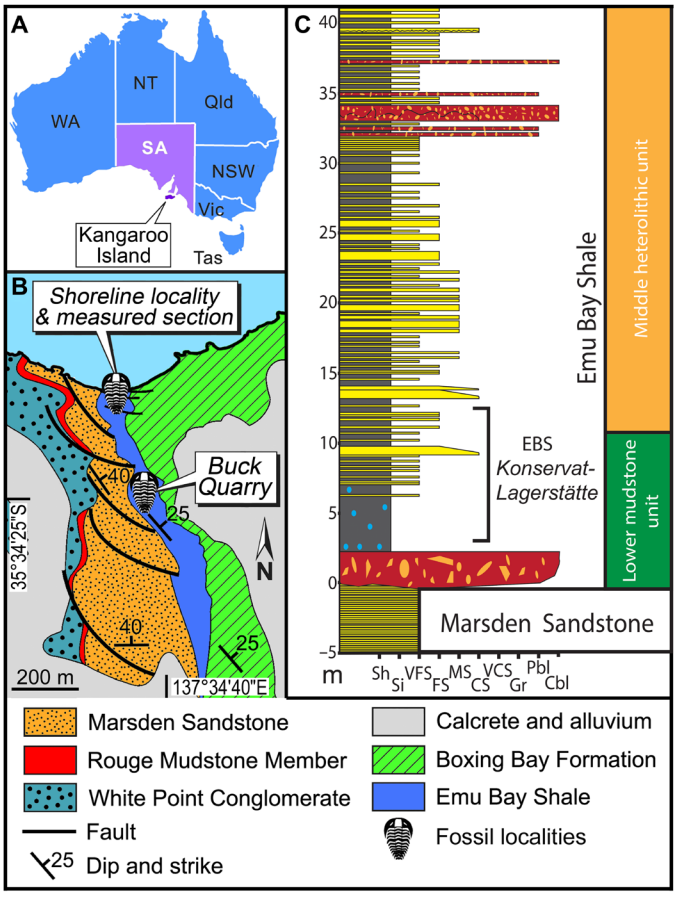

Fig. 1. Location and geologic context of the EBS. (**A**) Location map of Kangaroo Island in South Australia. (**B**) Geological map of Big Gully on the northeast coast of Kangaroo Island, after Gehling *et al.* (*11*) and García-Bellido *et al.* (*69*). (**C**) Stratigraphic column of the lower EBS at Big Gully showing the interval that preserves the Konservat-Lagerstätte.

within localized tectonic depressions in relatively deep water that was, at times, anoxic.

On the basis of a comprehensive outcrop and borehole study of the complete succession, we divide the EBS into three informal units: a 12-m-thick lower mudstone unit that includes a basal conglomerate, a 30-m-thick middle heterolithic unit comprising mudstone and sandstone with minor conglomerate, and a 32-m-thick top unit of interbedded siltstone and sandstone. The Konservat-Lagerstätte is found in a ~10-m-thick interval of the lower EBS that spans the gradational transition from the basal mudstone unit, dominated by shale, to the middle heterolithic unit, which is dominated by sandstone (Fig. 1C and fig. S2). Here, we focus our study on the lower and middle units.

Analysis of outcrop and borehole strata, in combination with polished slabs and thin sections, allows for a detailed reconstruction of paleoenvironments and depositional history. The base of the formation is marked by a ≤2.05-m-thick conglomerate bed with considerable local basal relief. The bed contains clasts of carbonate, basement vein quartz, sandstone, shale, and angular sandstone intraclasts of the directly underlying Marsden Sandstone. We concur with Gehling *et al.* (*11*) that the formation contact is a sequence boundary.

The lower mudstone unit is laminated at the <1-mm-scale (Fig. 2A), and bioturbation is absent (*14*). Soft-bodied fossils primarily exist in laminated mudstone that is dominated by clay but include thin (<0.5 mm) silt laminae and floating silt grains (Fig. 2, A, B, and K, and figs. S3 and S4); vetulicolians also exist in very fine sandstone beds (1 to 2 cm in thickness) intercalated with mudstone (fig. S4). In combination with evidence for transport of some soft-bodied forms (described below), the presence of floating silt grains suggests that mudstone was deposited from density-driven sediment gravity flows, e.g., (*28*). In the lower 7 m of the formation, small calcium phosphate nodules (5 to 10 mm) are locally abundant (Figs. 1C and 2B).

Geochemical attributes of samples collected from core are substantially different than those recovered from highly weathered outcrop samples. In particular, organic carbon (table S1) is far more abundant [up to 1.7% total organic carbon (TOC); average of 1.1%; $n = 40$] in core samples than previously reported for outcrop samples (<0.5% TOC) (*12*, *15*), and pyrite is present in concentrations up to 3.3 wt % (average of 1.0 wt %; table S1) but completely absent from surficial samples. In addition, the redox-sensitive trace element molybdenum is consistently enriched relative to composite shale standards (*29*, *30*) (enrichment factor of 2.3 to 11.6; average of 5.3; see Materials and Methods) in 93 samples measured from core (table S2), whereas enrichment factors of Mo for outcrop samples average <1 (*15*). We infer that these differences between relatively fresh borehole material and samples collected from surface exposures resulted from extensive weathering at the surface. Together, laminated shale with phosphate nodules, substantial concentrations of organic carbon and pyrite, and enrichment in Mo are characteristic of low-energy deposition in a relatively deep-water setting, with elevated primary productivity and oxygen depletion in the lower water column (*31*–*33*).

On the basis of the above data, we interpret the contact between the basal conglomerate and the overlying mudstone unit (Fig. 1C) to represent a major marine flooding surface. As such, the lower mudstone unit above this flooding surface represents much or all of a transgressive systems tract deposit. We posit that the mudstone is relatively devoid of sandstone due to sea level rise and shoreline retreat. In general, during sea level rise, sediment discharge is drastically reduced as bedload is deposited in alluvial channels and nearshore environments due to backwater effects (*34*). The laminated mudstone persists upward into the middle heterolithic unit, where it becomes volumetrically subordinate to coarser-grained lithologies.

The middle heterolithic unit (Fig. 1C) has numerous horizons with subaqueous mass transport features. Soft-sediment folds with consistent vergence range from the centimeter-scale to >1 m in thickness and deformed horizons up to 1 m in thickness commonly extend laterally for tens of meters (Fig. 2, C and D). The upper surface of one 25-cm-thick, parallel-laminated sandstone bed truncates the lamination, indicating that the upper surface is a slide scar produced by detachment and downslope movement of a mass of the bed (*35*, *36*). The middle unit also contains conglomerate in a wide variety of bed types (fig. S2). In some cases, pebbles to small cobbles are isolated along cryptic bedding surfaces within interbedded sandstone and shale (Fig. 2F). Three conspicuous beds of massive, ungraded, mud-supported conglomerate exhibit flat bases and consist of very poorly sorted clay to granule matrix with widely spaced, isolated, pebbles and cobbles up to ~20 cm across (Fig. 2E).

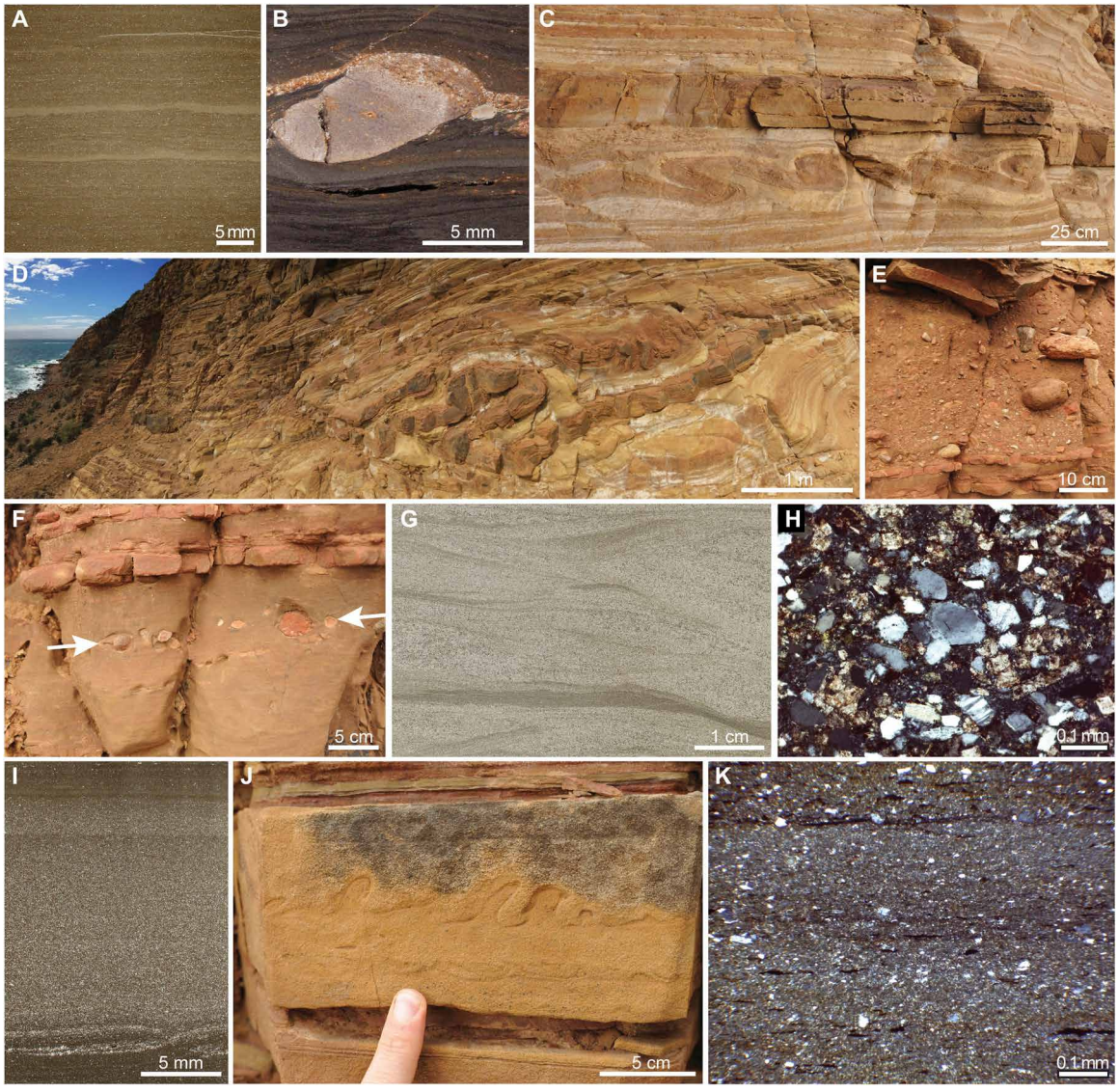

Fig. 2. Sedimentary attributes of the EBS in polished slab, outcrop, and thin section. Meterage refers to Fig. 1C. (**A**, **B**, and **K**) Laminated mudstones [(A) 7.5 m] include authigenic phosphate nodules [(B) 2.1 m] and abundant silt grains floating in a matrix [(K) 2.1 m]. (**C** and **D**) Slump folding [(C) 16 m and (D) 17.5 m]. (**E**) Paraconglomerate with large rounded-subrounded clasts (32.5 m). (**F**) Cobble-sized and pebble-sized clasts (arrows) in mudstone (31.9 m). (**G**) Rippled sand (light) with mud (dark) in ripple troughs (54.9 m). (**H** to **J**) Sandstones exhibit high matrix (dark) content, angular grains [(H) 17.2 m] and weak grading [(I) 6.4 m], with dewatering structures [(J) 27.8 m] common at bed bases.

Clast-supported conglomerate beds exhibit erosive bases, including a ≤95-cm-thick, channel fill pebble to cobble, conglomerate with a highly irregular, erosional base. Thinner pebble conglomerate channel fills also exist in the section, and some exhibit normal grading (fig. S2).

The features of the middle unit indicate remobilization and failure of the seafloor, gravity-driven transport, and deposition on relatively steep slopes. The verging, soft-sediment folds (Fig. 2, C and D) reflect deposition on a slope characterized by rapid accumulation of unconsolidated fine sediment (silt and clay) that was prone to failure, ductile deformation, and minor downslope movement (*37*). Common loading and dewatering structures provide further indication of high background accumulation rates of sediment and episodes of rapid deposition of coarse-grained sediment (Fig. 2J). The poorly sorted, mud-rich conglomerate beds with flat bases, dispersed cobbles, lack of grading, and massive texture (Fig. 2E) indicate a lack of flow turbulence and deposition from viscous debris flows. The conglomeratic channel fill beds with erosional bases record erosion by turbulent flows and subsequent deposition of coarse bedload. The array of mass transport, slump, and dewatering features in the middle unit indicate common liquefaction, high rates of sediment accumulation, episodic failure of the seafloor on a slope, and deposition of conglomeratic beds that ranged from viscous debris flows to turbulent mixed-bedload mass flows. This all suggests deposition in a more proximal (upslope) position than the lower mudstone unit, higher on the prodelta slope. Thus, the lower two units are interpreted to record shoaling and progradation of a deltaic system.

The upper 33-m-thick unit consists of parallel laminated siltstone and ripple-scale (~10 mm) cross-laminated fine to very fine sandstone (Fig. 2G). The basal 11 m of the upper unit is covered by alluvium, although a new core intercepted the contact between units. The transition in facies exposed in core is sharp. The upward coarsening trend in the underlying prodelta deposits is truncated at the base of the upper unit, and the latter does not have characteristics that would be expected for further progradation of a fan delta. Specifically, the upper unit is not composed of thicker and coarser delta front sandstone and conglomerate but instead comprises finely laminated siltstone to very fine sandstone (Fig. 2G). We thus interpret the base of the upper unit to likely be an unconformity surface with the upper part of the prograding deltaic system missing, presumably by erosion along a sequence boundary. The overlying, finely laminated upper unit would represent the transgressive systems tract deposits of the succeeding sequence.

DISCUSSION

An early Cambrian fan delta complex

The Kangaroo Island Group accumulated in an evolving continental rift system (*10*, *23*, *25*). The EBS is similar to other units of the group in that petrologic data (angular grains, abundant lithic grains, and detrital micas; Fig. 2H) indicate a proximal sedimentary source area where rates of physical weathering outstripped those of chemical weathering, typical of tectonically active settings and arid climates, e.g., (*38*). Yet, the EBS is distinct within the Kangaroo Island Group in that it records deposition in moderately deep water, as evidenced by laminated pyritic mudstone with authigenic phosphate nodules, and geochemical indicators of anoxia (tables S1 and S2). The overall sedimentary succession of the EBS indicates that a relatively rapid transgression above its basal conglomerate led to the development of a low-energy muddy basin (*11*). Relative sea level was likely mostly driven by abrupt subsidence linked to active tectonics, although a eustatic rise of ~80 m is also estimated for the base of Cambrian Stage 4 (*39*). The resulting lower mudstone unit was succeeded by the ~35-m-thick upward-coarsening middle unit that records distal-to-proximal prodelta facies. Although thickness cannot be used for a direct estimate of water depth, because of load-induced subsidence, eustasy, compaction, and other factors, the ~42-m-thick prodelta section (lower and middle units) would suggest likely water depths for the lower mudstone in the range of ~50 to 100 m. Soft-sediment deformation features and associated mass transport deposits can form on deltas with slopes as low as 1° (*40*, *41*), but the presence of debrites and channel deposits with clasts up to cobble size would suggest steeper slopes and close proximity to range-bounding faults (*42*). Thus, the EBS likely represents the lower part of the subaqueous section of a fan delta complex.

A prodelta interpretation for the lower and middle units of EBS is supported by evidence for rapid deposition and frequent failures of the seafloor, which includes the high abundance of slump folds with consistent vergence, slide scars, dewatering structures, and debris flows in the middle heterolithic unit (Fig. 1C) (*43*–*50*). The mudstone beds, including those that contain the Konservat-Lagerstätte, include angular silt grains with abundant clay matrix and no traction features (Fig. 2K), which, in the overall depositional context, would suggest deposition from the collapse of hypopycnal flows, sediment plumes that were initially suspended within a buoyant freshwater lens at the river's mouth (*51*, *52*). Textural properties of fine sandstone and siltstone beds of the middle unit—particularly the poor sorting and high matrix content (Fig. 2, H and I)—suggest likely deposition from sediment flows initiated by turbid plumes at the mouth of the river that fed the delta (*51*, *53*). The massive and parallel-laminated sandstone beds, the latter recording upper plane bed flows, suggest event deposition, likely from high-concentration hyperpycnal flows that discharged directly from the river's mouth across the sloping seafloor of the delta front during peak flow events (*50*, *53*).

The EBS biota was preserved in a nearshore but relatively deep-water (tens of meters) setting representing the prodelta of a fan delta complex that developed in a tectonically active basin. The preservation of abundant, delicate, soft-bodied organisms in a fan delta setting that was subject to high-energy depositional events (e.g., debris flows) is unexpected. However, the muddy, lower prodelta setting inferred for the lower EBS (Fig. 1C) provided similar biostratinomic conditions to those of other BST deposits, specifically (i) entrainment of organisms in sediment gravity flows, (ii) their downslope transportation across chemical gradients, and (iii) their rapid burial in muddy sediment (*8*). Petrographic evidence, including millimeter-scale mudstone laminae that are ungraded yet contain abundant silt and very fine sand grains "floating" within a clay matrix (Fig. 2K), indicate rapid deposition and little sustained traction transport. This suggests that many of the organisms recovered from the EBS lower mudstone unit were episodically transported by downwelling flows, likely created by collapse of sediment plumes at the river's mouth (*51*, *54*). Such density-driven flows are set up by episodic fluvial discharge into the basin (i.e., floods) or by remobilization and short-distance, gravity-driven transport of mud that initially accumulated on the upper prodelta.

Paleoenvironmental influence on the EBS biota

These findings expand the known range of paleoenvironmental settings for exceptional preservation in the Cambrian. BST deposits, the most abundant type of Cambrian Lagerstätten, characteristically occur in offshore shelf and slope settings (*8*). Although the early Cambrian Chengjiang BST deposit has historically been interpreted as a distal shelf succession (*55*), its depositional environment was recently reinterpreted as a distal deltaic environment (*56*). In contrast to the localized fan delta setting of the EBS, the fossil-bearing outcrops of the Chengjiang span a broad outcrop area (>80 km) that was located 20 to 50 km offshore (*57*, *58*). Thus, the fan delta setting of the EBS represents a fundamentally different, more proximal environmental setting. The paleoenvironment of the EBS is clearly differentiated from the Chengjiang and also from other Cambrian Lagerstätten because the EBS biota proliferated and was preserved in a nearshore setting within a narrow seaway in a highly localized, tectonically active rift basin that was influenced by high-energy depositional events, including coarse-grained debris flows.

The exceptional depositional setting of the EBS provides a platform for understanding the composition of its biota relative to those of other Cambrian Lagerstätten. Like BST deposits, the EBS was prone to anoxia in benthic environments where conditions conducive to exceptional preservation were favored (*8*, *59*–*61*). Elevated primary productivity, consistent with substantial organic and pyrite contents and the formation of authigenic phosphate nodules in EBS mudstone (Fig. 2B), may have played a large role in sustaining the ecosystem. Geochemical data (tables S1 and S2) suggest that respiration of exported organic matter at the seafloor or in the lower water column created an oxygen demand, leading to episodic anoxia in

the prodelta setting, thereby imposing an environmental barrier upon the benthos. This contrasts with recent claims that the EBS mudstone hosting the Konservat-Lagerstätte accumulated under oxygenated bottom waters (*12*, *15*). In addition to redox instability in the prodelta, overall conditions of the EBS fan delta system presented other challenges to benthic colonization, likely including a soft, perhaps soupy, substrate, suggested by abundant dewatering structures (Fig. 2J and fig. S4)—contrasting sharply with evidence for firm substrates in BST deposits (*8*)—as well as episodic high turbidity and potential variations in salinity around the zone of freshwater mixing, given the nearshore setting.

Analysis of a new dataset of >25,000 fossil occurrences from the EBS Konservat-Lagerstätte (Figs. 3 and 4, and table S3) reveals that the biota was strongly influenced by these environmental factors. We hypothesize that most taxa were transported to the prodelta setting, although evidence of trilobite moult assemblages (*62*, *63*) suggests periodic colonization of the benthic environment by a low diversity community. The most abundant taxon is the trilobite *Estaingia bilobata* (Fig. 3D), which constitutes over 80% of all individuals in the biota (Fig. 3A) and locally exists in densities of >600 individuals/m^2 (*64*). This species, along with the trilobite *Redlichia takooensis* (*65*, *66*) and the enigmatic soft-bodied, multielement organism informally referred to as "petalloid" (*14*), represent the most abundant epibenthic constituents of the EBS biota, which is otherwise marked by a low diversity of epibenthic forms (Fig. 3, A to C, and table S3). The extreme abundance of *E. bilobata* in the prodelta setting suggests that this species was an exaerobic zone specialist that thrived under oxygen conditions too low to support other contemporaneous species (*14*), similar to the middle Cambrian trilobite *Elrathia kingii* (*67*). The abundance of the other two taxa implies that they may have been tolerant of dysoxic conditions. We infer that the trilobite/petalloid prodelta assemblage may have been preserved in situ within the Konservat-Lagerstätte interval (Fig. 5), as supported by paleoecologic and biostratinomic data, including common molt ensembles of both trilobite species (*62*, *63*), the full range of *E. bilobata* growth stages (*64*, *68*), and articulated specimens of petalloids. The endobenthic palaeoscolecid worm *Wronascolex antiquus* is also common (table S3) (*69*). Individuals of this taxon appear to have been transported downslope from their

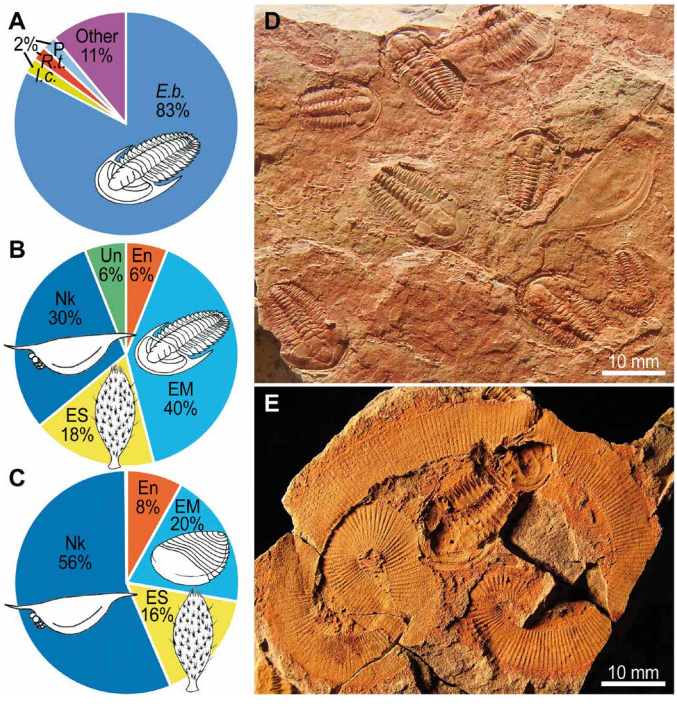

Fig. 3. Relative abundance and diversity of the EBS biota. (**A**) Relative abundance of EBS species (% of individuals; *n* = 25,260). (**B**) Relative diversity of species (*n* = 50) based on life mode. (**C**) Relative abundance of individuals (*n* = 4380; excluding *E. bilobata*) based on life mode. (**D**) Typical fossil slab showing *E. bilobata* and *I. communis*. (**E**) Coiled specimen of *W. antiquus* preserved prone with *E. bilobata* (SAMA P15051b). Abbreviations: *E.b.*, *E. bilobata*; *I.c.*, *I. communis*; *R.t.*, *R. takooensis*; P, petalloid; En, endobenthic; EM, epibenthic mobile; ES, epibenthic sessile; Nk, nektonic; Un, unknown.

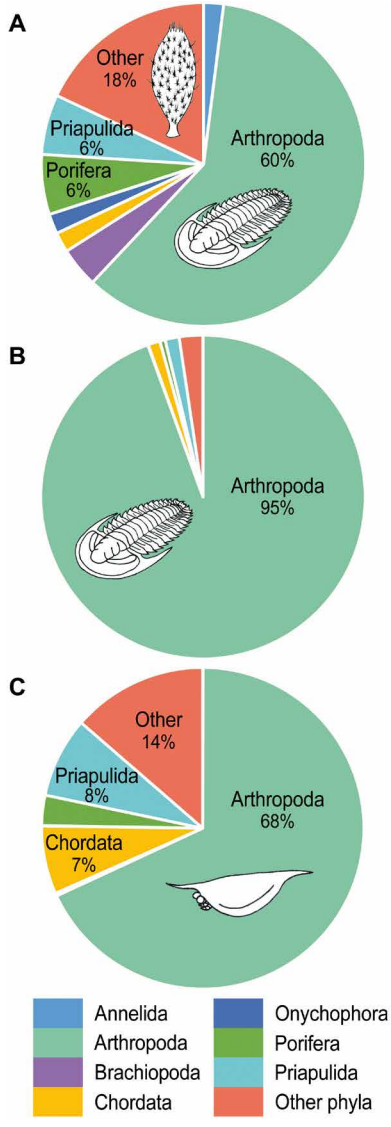

Fig. 4. Relative diversity and abundance of phyla within the EBS Konservat-Lagerstätte interval at Big Gully. (**A**) Relative diversity of species (*n* = 50). (**B**) Relative abundance of total individuals sampled (*n* = 25,260). (**C**) Relative abundance of individuals sampled, excluding *E. bilobata* (*n* = 4380).

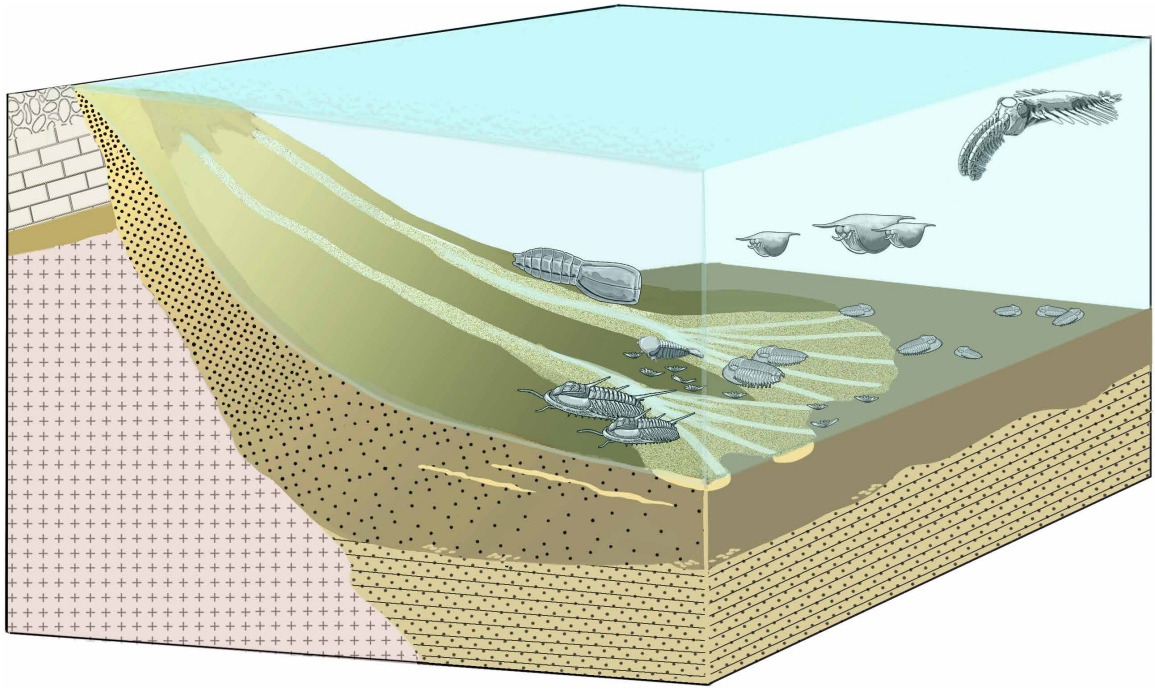

Fig. 5. Artist's reconstruction of the paleoenvironmental setting of the EBS during the deposition of the Konservat-Lagerstätte interval, with some common members of the biota. From left to right, fossils represented are *N. aldridgei* (vetulicolian), *R. takooensis* (trilobite), *W. barbarahardyae* (megacheiran), petalloid (unknown affinity), *E. bilobata* (trilobite), *I. communis* (bivalved arthropod), and *E. briggsi* (radiodont).

living environments because specimens of *W. antiquus*, like those of all other infaunal taxa, are found exclusively prone along bedding planes of unbioturbated strata of the lower prodelta (Fig. 3E) rather than in burrows (*70*, *71*). Transportation of all infaunal taxa represented in the EBS is also supported by the absence of bioturbation from the Lagerstätte interval, except for two isolated examples of small traces associated with eldonioid carcasses (*72*).

The remaining and much rarer endobenthic and epibenthic species (Fig. 3, B and C) were likely transported from habitats upslope. For example, the emuellid trilobite *Balcoracania dailyi* proliferated in tidally influenced, marginal marine settings where it lived in great abundance (*73*), suggesting that the extremely rare occurrences of this taxon in the EBS Lagerstätte interval represent individuals transported from much shallower waters near the shoreline. Elevated turbidity, episodic perturbation by high-energy depositional events, and substrate instability—particularly on the prodelta—are likely responsible for the rarity of filter-feeding benthos, whether sessile or facultatively mobile. Notably, echinoderms are absent, and groups such as brachiopods, chancelloriids, and hyoliths are rare (table S3) (*14*, *74*) and typically found as disarticulated elements. The absence of echinoderms may be explained by a lack of suitable firm substrates and/or terrestrial freshwater runoff into the delta system as modern forms are typically stenohaline (*75*). Sponges, with the exception of leptomitids, are very rare and are low in diversity. This contrasts markedly with BST deposits, where benthic filter feeders tend to be more diverse and abundant (*76*–*79*).

A diverse and relatively abundant nektonic community preserved within the EBS (Fig. 3, B and C) indicates that the upper water column was well oxygenated and largely unaffected by adverse benthic conditions. Arthropods such as *Echidnacaris briggsi*, *Isoxys communis*, *Myoscolex ateles*, *Tuzoia australis*, and *Wisangocaris barbarahardyae*, in addition to the vetulicolian *Nesonektris aldridgei*, inhabited the water column above the prodelta and delta front settings (Fig. 5). The "bivalved" arthropods *I. communis* and *T. australis*, plus the radiodont *E. briggsi*, would have regularly molted their exoskeletons, and subsequently, their exuviae would have sunk to the seafloor (*14*), as evidenced by empty bivalved carapaces (*80*) and isolated body parts of *E. briggsi*, especially frontal appendages and oral cones (*7*, *81*, *82*). A similar scenario has been suggested for arthropod molt remains from the Burgess Shale (*83*). The arthropod *W. barbarahardyae* may have visited the benthos to feed on *E. bilobata*—as shown by cololites (*84*, *85*)—and swimming individuals of the vetulicolian *N. aldridgei* appear to have been occasionally swept up by sediment gravity flows that buried them in silt and fine sand (*14*, *86*). This suggests that both *W. barbarahardyae* and *N. aldridgei* may have spent time near the seafloor, either on the delta front or on the prodelta during times when oxygen levels were favorable.

The EBS biota inhabited a fan delta complex within a tectonically active, nearshore basin—a setting that contrasts greatly with the offshore shelf and slope environments of other Cambrian Lagerstätten. Overall, deltaic sedimentation processes, coupled with fluctuating oxygen conditions in the distal prodelta setting, strongly influenced the distinctive benthic community structure of the EBS biota. Episodic high-energy events and turbidity appear to have been prohibitive to the development of a diverse filter-feeding benthos, but these conditions aided downslope transportation and rapid burial of many benthic species. Redox fluctuations in the prodelta environment may have also restricted the in situ benthos to low-oxygen specialists, such as the trilobite *E. bilobata*, but episodes of anoxia may have served to promote exceptional preservation of the entire community,

as in other Cambrian Lagerstätten (*87*). The absence of firm substrates that are characteristic of other Cambrian BST deposits appears to have presented additional challenges to sessile and facultatively mobile benthos. Conversely, a diverse and abundant nektonic community comprising taxa typical of other Cambrian Lagerstätten indicates that the upper water column was well oxygenated and largely divorced from near seafloor conditions across the delta complex. The environmental setting of the EBS is fundamentally unique among exceptionally preserved biotas of the Cambrian and appears to have played a significant role in shaping the community, including the substantial number and relatively high proportion of endemic taxa (~70% of genera; table S3) (*9*), that inhabited the early Cambrian fan delta complex. The EBS expands the known environmental range for preservation of soft-bodied macrofossil assemblages in the Cambrian and reveals that the distinctive environmental setting of the EBS controlled the composition of the community and facilitated exceptional preservation of this Gondwanan fossil assemblage in the immediate aftermath of the Cambrian explosion.

MATERIALS AND METHODS

Stratigraphic and sedimentological data

The EBS was measured and logged in centimeter-scale detail at its only complete exposure in sea cliffs immediately adjacent to Big Gully (*11*) (fig. S1) and at smaller stratigraphic exposures in two nearby fossil quarries (*14*). Broad horizontal exposure allowed us to correlate across numerous small faults, with the aid of a Brunton compass and laser rangefinder with an inclinometer. Oriented rock samples were taken at regular intervals, from which polished slabs and 49 thin sections were prepared and analyzed by petrographic microscope. A suite of samples and thin sections were also prepared from a continuously sampled 40-cm interval from Buck Quarry. Optical microscopy was augmented with scanning electron microscopy–energy-dispersive x-ray spectroscopy analyses using a Hitachi SU-70 field-emission scanning electron microscope and a Bruker energy-dispersive x-ray spectrometer at Pomona College. A borehole drilled at Big Gully in January 2017 was studied to augment the data collected from outcrop.

TOC and weight % pyrite sulfur were measured from 40 borehole samples using an Elementar Vario Micro Cube elemental analyzer at Pomona College. Sample powders were treated with 1 M HCl to remove calcium carbonate then rinsed three times in deionized H_2O, dried, and disaggregated prior to analysis. Major and trace element chemistry of 93 samples from the Konservat-Lagerstätte interval was determined using a Panalytical Axios XRF spectrometer at Pomona College. Samples were crushed to powder using a Rocklabs shatterbox equipped with a tungsten-carbide grinding head and prepared as twice-fused borosilicate glass beads following the method of Johnson *et al.* (*88*). Concentrations of the trace element Mo were normalized to Al and compared to average shale values from (*29*, *30*) to determine enrichment factors, using the following equation of (*32*)

$$EF_{Mo} = Mo / Al_{SAMPLE} / Mo / Al_{AVERAGE\ SHALE}$$

Faunal data

Fossils from the EBS Konservat-Lagerstätte were first found in 1954 along the shoreline immediately east of the mouth of Big Gully. For over 50 years, the EBS exposures on the shoreline rock platform and adjacent cliffs at this site were the primary sources of material for study (*89*, *90*). In September 2007, Buck Quarry was opened to the south and has yielded most of the specimens documented in recent studies, including much of the data provided herein. In September 2012, a second, smaller excavation (Daily Quarry) between Buck Quarry and the shoreline locality was opened and has also produced a similar faunal assemblage, although collecting has been less extensive than at Buck Quarry.

The specimens from Buck Quarry were collected from a 6.4-m interval (levels 9.2 to 15.6) in the lower part of the EBS; the most productive beds are between levels 9.8 and 12.6. During field seasons between 2007 and 2017, all complete or identifiable fossils were collected (especially soft-bodied taxa), although not all specimens of the trilobite *E. bilobata* were kept due to their extreme abundance; subsequent field work in 2018 and 2019 was more targeted to collecting new or rare taxa. Where possible, both part and counterpart of each fossil was kept, labeled, and cataloged. The same collecting methods were followed for the equivalent fossiliferous interval along strike in Daily Quarry.

The faunal information presented here is based on the entire collection of specimens from the EBS Konservat-Lagerstätte housed in the South Australian Museum (Adelaide) collected before 2018 (table S3). This represents a dataset comprising ~5800 registered fossils, in addition to associated unregistered specimens, from the three key sites at Big Gully: Buck Quarry, Daily Quarry, and the shoreline locality. These data were used to determine the overall relative diversity and abundance of taxa (Figs. 3A and 4) and their life modes (Fig. 3, B and C). Life mode includes information on tiering and mobility only—following similar categories used in previous studies, e.g., (*76*, *77*, *91*–*93*)—as feeding habits (e.g., suspension/filtering, deposit, hunting/scavenging, and grazing) are largely unknown for many EBS species. In addition to references cited above, references (*94*–*110*) pertain to data in table S3.

Supplementary Materials

This PDF file includes:

Figs. S1 to S4
Tables S1 to S3

REFERENCES AND NOTES

1. D. H. Erwin, M. Laflamme, S. M. Tweedt, E. A. Sperling, D. Pisani, K. J. Peterson, The Cambrian conundrum: Early divergence and later ecological success in the early history of animals. *Science* **334**, 1091–1097 (2011).
2. D. E. G. Briggs, The Cambrian explosion. *Curr. Biol.* **25**, R864–R868 (2015).
3. J. R. Paterson, G. D. Edgecombe, M. S. Lee, Trilobite evolutionary rates constrain the duration of the Cambrian explosion. *Proc. Natl. Acad. Sci. U.S.A.* **116**, 4394–4399 (2019).
4. D. E. Briggs, C. Nedin, The taphonomy and affinities of the problematic fossil Myoscolex from the Lower Cambrian Emu Bay Shale of South Australia. *J. Paleontol.* **71**, 22–32 (1997).
5. M. S. Lee, J. B. Jago, D. C. García-Bellido, G. D. Edgecombe, J. G. Gehling, J. R. Paterson, Modern optics in exceptionally preserved eyes of Early Cambrian arthropods from Australia. *Nature* **474**, 631–634 (2011).
6. J. R. Paterson, D. C. García-Bellido, M. S. Y. Lee, G. A. Brock, J. B. Jago, G. D. Edgecombe, Acute vision in the giant Cambrian predator *Anomalocaris* and the origin of compound eyes. *Nature* **480**, 237–240 (2011).
7. J. R. Paterson, G. D. Edgecombe, D. C. García-Bellido, Disparate compound eyes of Cambrian radiodonts reveal their developmental growth mode and diverse visual ecology. *Sci. Adv.* **6**, eabc6721 (2020).
8. R. R. Gaines, "Burgess Shale-type preservation and its distribution in space and time" in *Reading and Writing of the Fossil Record: Preservational Pathways to Exceptional Fossilization*, vol. 20 of *The Paleontological Society Papers*, M. Laflamme, J. D. Schiffbauer, S. A. F. Darroch, Eds. (The Paleontological Society, 2014), pp. 123–146.
9. J. D. Holmes, D. C. García-Bellido, M. S. Lee, Comparisons between Cambrian Lagerstätten assemblages using multivariate, parsimony and Bayesian methods. *Gondwana Res.* **55**, 30–41 (2018).

10. B. Daily, P. S. Moore, B. R. Rust, Terrestrial-marine transition in the Cambrian rocks of Kangaroo Island, South Australia. *Sedimentology* **27**, 379–399 (1980).
11. J. G. Gehling, J. B. Jago, J. R. Paterson, D. C. García-Bellido, G. D. Edgecombe, The geological context of the lower Cambrian (Series 2) Emu Bay shale lagerstätte and adjacent stratigraphic units, Kangaroo Island, South Australia. *Aust. J. Earth Sci.* **58**, 243–257 (2011).
12. P. A. Hall, D. M. McKirdy, G. P. Halverson, J. B. Jago, J. G. Gehling, Biomarker and isotopic signatures of an early Cambrian Lagerstätte in the Stansbury Basin, South Australia. *Org. Geochem.* **42**, 1324–1330 (2011).
13. D. M. McKirdy, P. A. Hall, C. Nedin, G. P. Halverson, B. H. Michaelsen, J. B. Jago, J. G. Gehling, R. J. F. Jenkins, Paleoredox status and thermal alteration of the lower Cambrian (series 2) Emu Bay Shale Lagerstätte, South Australia. *Aust. J. Earth Sci.* **58**, 259–272 (2011).
14. J. R. Paterson, D. C. García-Bellido, J. B. Jago, J. G. Gehling, M. S. Y. Lee, G. D. Edgecombe, The Emu Bay Shale Konservat-Lagerstätte: A view of Cambrian life from East Gondwana. *J. Geol. Soc. London* **173**, 1–11 (2016).
15. P. A. Hall, D. M. McKirdy, G. P. Halverson, J. B. Jago, A. S. Collins, Biogeochemical status of the Paleo-Pacific Ocean: Clues from the early Cambrian of South Australia. *Aust. J. Earth Sci.* **68**, 968–991 (2021).
16. J. W. Hagadorn, R. H. Dott Jr., D. Damrow, Stranded on a Late Cambrian shoreline: Medusae from central Wisconsin. *Geology* **30**, 147–150 (2002).
17. E. Mayoral, E. Liñán, J. A. G. Vintaned, F. Muñiz, R. Gozalo, Stranded jellyfish in the lowermost Cambrian (Corduban) of Spain. *Span. J. Palaeont.* **19**, 191–198 (2021).
18. A. Sappenfield, L. G. Tarhan, M. L. Droser, Earth's oldest jellyfish strandings: A unique taphonomic window or just another day at the beach? *Geol. Mag.* **154**, 859–874 (2017).
19. J. H. Collette, J. W. Hagadorn, Three-dimensionally preserved arthropods from Cambrian Lagerstätten of Quebec and Wisconsin. *J. Paleontol.* **84**, 646–667 (2010).
20. E. B. Naimark, A. V. Sizov, V. B. Khubanov, "Kimiltei is a new Late Cambrian Lagerstätte with the faunistic complex of arthropods (Euthycarcinoidae, Synziphosurina, and Chasmataspidida) in the Irkutsk region" in *Doklady Earth Sciences* (Springer, 2023), vol. 512, pp. 859–870.
21. B. J. Slater, Life in the Cambrian shallows: Exceptionally preserved arthropod and mollusk microfossils from the early Cambrian of Sweden. *Geology* **52**, 256–260 (2024).
22. R. Vaucher, E. L. Martin, H. Hormière, B. Pittet, A genetic link between Konzentrat-and Konservat-Lagerstätten in the Fezouata Shale (lower Ordovician, Morocco). *Palaeogeogr. Palaeoclimatol. Palaeoecol.* **460**, 24–34 (2016).
23. R. J. Jenkins, M. Sandiford, Observations on the tectonic evolution of the southern Adelaide Fold Belt. *Tectonophysics* **214**, 27–36 (1992).
24. D. I. Gravestock, C. G. Gatehouse, "Stansbury Basin" in *The Geology of South Australia, Volume 2: The Phanerozoic*, vol. 54 of *South Australia Geologic Survey Bulletin* (Mines and Energy, South Australia, Geological Survey of South Australia, 1995), pp. 5–19.
25. T. Flöttmann, P. Haines, J. Jago, P. James, A. Belperio, J. Gum, Formation and reactivation of the Cambrian Kanmantoo Trough, SE Australia: Implications for early Palaeozoic tectonics at eastern Gondwana's plate margin. *J. Geol. Soc. London* **155**, 525–539 (1998).
26. J. B. Jago, C. J. Bentley, J. R. Paterson, J. D. Holmes, T. R. Lin, X. W. Sun, The stratigraphic significance of early Cambrian (Series 2, Stage 4) trilobites from the Smith Bay Shale near Freestone Creek, Kangaroo Island. *Aust. J. Earth Sci.* **68**, 204–212 (2021).
27. P. M. Myrow, J. W. Goodge, G. A. Brock, M. J. Betts, T. Y. S. Park, N. C. Hughes, R. R. Gaines, Tectonic trigger to the first major extinction of the Phanerozoic: The early Cambrian Sinsk event. *Sci. Adv.* **10**, eadl3452 (2024).
28. S. E. Gabbott, J. Zalasiewicz, D. Collins, Sedimentation of the Phyllopod Bed within the Cambrian Burgess Shale Formation of British Columbia. *J. Geol. Soc. London* **165**, 307–318 (2008).
29. K. H. Wedepohl, Environmental influences on the chemical composition of shales and clays. *Phys. Chem. Earth* **8**, 307–333 (1971).
30. K. H. Wedepohl, "The composition of the upper Earth's crust and the natural cycles of selected metals. Metals in raw materials, natural resources" in *Metals and Their Compounds in the Environment: Occurrence, Analysis and Biological Relevance* (John Wiley and Sons, 1991), pp. 3-17.
31. S. J. Schenau, C. P. Slomp, G. J. De Lange, Phosphogenesis and active phosphorite formation in sediments from the Arabian Sea oxygen minimum zone. *Mar. Geol.* **169**, 1–20 (2000).
32. N. Tribovillard, T. J. Algeo, T. Lyons, A. Riboulleau, Trace metals as paleoredox and paleoproductivity proxies: An update. *Chem. Geol.* **232**, 12–32 (2006).
33. Y. Xiong, R. Guilbaud, C. L. Peacock, R. P. Cox, D. E. Canfield, M. D. Krom, S. W. Poulton, Phosphorus cycling in Lake Cadagno, Switzerland: A low sulfate euxinic ocean analogue. *Geochim. Cosmochim. Acta* **251**, 116–135 (2019).
34. C. Wu, J. A. Nitterour, Impacts of backwater hydrodynamics on fluvial–deltaic stratigraphy. *Basin Res.* **32**, 567–584 (2020).
35. P. M. Myrow, J. Chen, Estimates of large magnitude Late Cambrian earthquakes from seismogenic soft-sediment deformation structures: Central Rocky Mountains. *Sedimentology* **62**, 621–644 (2015).
36. W. Li, J. Chen, A. J. Hakim, P. M. Myrow, Middle Ordovician mass-transport deposits from western Inner Mongolia, China: Mechanisms and implications for basin evolution. *Sedimentology* **69**, 1301–1338 (2022).
37. P. M. Myrow, W. Fischer, J. W. Goodge, Wave-modified turbidites: Combined-flow shoreline and shelf deposits, Cambrian, Antarctica. *J. Sediment. Res.* **72**, 641–656 (2002).
38. R. V. Ingersoll, Actualistic sandstone petrofacies: Discriminating modern and ancient source rocks. *Geology* **18**, 733–736 (1990).
39. B. U. Haq, S. R. Schutter, A chronology of Paleozoic sea-level changes. *Science* **322**, 64–68 (2008).
40. J. M. Coleman, H. J. Walker, W. E. Grabau, Sediment instability in the Mississippi River delta. *J. Coast. Res.* **14**, 872–881 (1998).
41. J. M. Maloney, S. J. Bentley, K. Xu, J. Obelcz, I. Y. Georgiou, N. H. Jafari, M. D. Miner, Mass wasting on the Mississippi River subaqueous delta. *Earth Sci. Res.* **200**, 103001 (2020).
42. J. G. McPherson, G. Shanmugam, R. J. Moiola, Fan-deltas and braid deltas: Varieties of coarse-grained deltas. *Geol. Soc. Am. Bull.* **99**, 331–340 (1987).
43. D. B. Prior, B. D. Bornhold, J. M. Coleman, W. R. Bryant, Morphology of a submarine slide, Kitimat Arm, British Columbia. *Geology* **10**, 588–592 (1982).
44. W. Nemec, R. J. Steel, S. J. Poreebski, Å. Spinnangr, "Domba Conglomerate, Devonian, Norway: Process and lateral variability in a mass flow-dominated, lacustrine fan-delta" in *Sedimentology of Gravels and Conglomerates* (Canadian Society of Petroleum Geologists, 1984), pp. 295–320.
45. W. Nemec, "Aspects of sediment movement on steep delta slopes" in *Coarse-Grained Deltas* (John Wiley and Sons, 1990), pp. 29–73.
46. G. Postma, "Depositional architecture and facies of river and fan deltas: A synthesis" in *Coarse-Grained Deltas* (John Wiley and Sons, 1990), pp. 13–28.
47. P. M. Myrow, R. N. Hiscott, Shallow-water gravity-flow deposits, Chapel Island Formation, Southeast Newfoundland, Canada. *Sedimentology* **38**, 935–959 (1991).
48. B. K. Horton, J. G. Schmitt, Sedimentology of a lacustrine fan-delta system, Miocene Horse Camp Formation, Nevada, USA. *Sedimentology* **43**, 133–155 (1996).
49. M. P. Lamb, P. M. Myrow, C. Lukens, K. Houck, J. Strauss, Deposits from wave-influenced turbidity currents: Pennsylvanian Minturn Formation, Colorado, USA. *J. Sediment. Res.* **78**, 480–498 (2008).
50. P. M. Myrow, C. Lukens, M. P. Lamb, K. Houck, J. Strauss, Dynamics of a transgressive prodeltaic system: Implications for geography and climate within a Pennsylvanian intracratonic basin, Colorado, USA. *J. Sediment. Res.* **78**, 512–528 (2008).
51. C. Zavala, S. X. Pan, Hyperpycnal flows and hyperpycnites: Origin and distinctive characteristics. *Lithol. Reserv.* **30**, 1–27 (2018).
52. C. Zavala, M. Arcuri, M. Di Meglio, A. Zorzano, G. Otharán, A. Irastorza, A. Torresi, Deltas: A new classification expanding Bates's concepts. *J. Palaeogeogr.* **10**, 1–15 (2021).
53. C. Zavala, Hyperpycnal (over density) flows and deposits. *J. Palaeogeogr.* **9**, 1–21 (2020).
54. J. D. Parsons, J. W. Bush, J. P. Syvitski, Hyperpycnal plume formation from riverine outflows with small sediment concentrations. *Sedimentology* **48**, 465–478 (2001).
55. M. Y. Zhu, J. M. Zhang, G. X. Li, Sedimentary environments of the Early Cambrian Chengjiang Biota: Sedimentology of the Yu'anshan Formation in Chengjiang county, eastern Yunnan. *Acta Palaeontol. Sin.* **40**, 80–105 (2001).
56. F. Saleh, C. Qi, L. A. Buatois, M. G. Mángano, M. Paz, R. Vaucher, Q. Zheng, X.-G. Hou, S. E. Gabbott, X. Ma, The Chengjiang Biota inhabited a deltaic environment. *Nat. Commun.* **13**, 1569 (2022).
57. X. Zhang, W. Liu, Y. Zhao, Cambrian Burgess Shale-type Lagerstätten in south China: Distribution and significance. *Gondwana Res.* **14**, 255–262 (2008).
58. X.-G. Hou, D. J. Siveter, D. J. Siveter, R. J. Aldridge, P. Cong, S. E. Gabbott, X. Ma, M. A. Purnell, M. Williams, *The Cambrian Fossils of Chengjiang, China: The Flowering of Early Animal Life* (John Wiley and Sons, 2017).
59. P. A. Allison, C. E. Brett, In situ benthos and paleo-oxygenation in the middle Cambrian Burgess Shale, British Columbia, Canada. *Geology* **23**, 1079–1082 (1995).
60. N. J. Butterfield, Secular distribution of Burgess-Shale-type preservation. *Lethaia* **28**, 1–13 (1995).
61. E. U. Hammarlund, R. R. Gaines, M. G. Prokopenko, C. Qi, X.-G. Hou, D. E. Canfield, Early Cambrian oxygen minimum zone-like conditions at Chengjiang. *Earth Planet. Sci. Lett.* **475**, 160–168 (2017).
62. H. B. Drage, J. D. Holmes, D. C. García-Bellido, A. C. Daley, An exceptional record of Cambrian trilobite moulting behaviour preserved in the Emu Bay Shale, South Australia. *Lethaia* **51**, 473–492 (2018).
63. H. B. Drage, J. D. Holmes, D. C. García-Bellido, J. R. Paterson, Associations between trilobite intraspecific moulting variability and body proportions: *Estaingia bilobata* from the Cambrian Emu Bay Shale, Australia. *Palaeontology* **66**, e12651 (2023).
64. J. D. Holmes, J. R. Paterson, D. C. García-Bellido, The post-embryonic ontogeny of the early Cambrian trilobite *Estaingia bilobata* from South Australia: Trunk development and phylogenetic implications. *Pap. Palaeontol.* **7**, 931–950 (2021).
65. J. D. Holmes, J. R. Paterson, D. C. García-Bellido, The trilobite *Redlichia* from the lower Cambrian Emu Bay Shale Konservat-Lagerstätte of South Australia: Systematics, ontogeny and soft-part anatomy. *J. Syst. Palaeontol.* **18**, 295–334 (2020).

66. R. D. Bicknell, J. D. Holmes, S. Pates, D. C. García-Bellido, J. R. Paterson, Cambrian carnage: Trilobite predator-prey interactions in the Emu Bay Shale of South Australia. *Palaeogeogr. Paleoclimatol. Palaeoecol.* **591**, 110877 (2022).
67. R. R. Gaines, M. L. Droser, Paleoecology of the familiar trilobite *Elrathia kingii*: An early exaerobic zone inhabitant. *Geology* **31**, 941–944 (2003).
68. J. D. Holmes, J. R. Paterson, D. C. García-Bellido, Complex axial growth patterns in an early Cambrian trilobite from South Australia. *Proc. R. Soc. B* **288**, 20212131 (2021).
69. D. C. García-Bellido, J. R. Paterson, G. D. Edgecombe, Cambrian palaeoscolecids (Cycloneuralia) from Gondwana and reappraisal of species assigned to *Palaeoscolex*. *Gondwana Res.* **24**, 780–795 (2013).
70. D. Huang, J. Chen, M. Zhu, F. Zhao, The burrow dwelling behavior and locomotion of palaeoscolecidian worms: New fossil evidence from the Cambrian Chengjiang fauna. *Palaeogeogr. Paleoclimatol. Palaeoecol.* **398**, 154–164 (2014).
71. Y. Yang, X. Zhang, Y. Zhao, Y. Qi, L. Cui, New paleoscolecid worms from the early Cambrian north margin of the Yangtze Platform, South China. *J. Paleontol.* **92**, 49–58 (2018).
72. N. I. Schroeder, J. R. Paterson, G. A. Brock, Eldonioids with associated trace fossils from the lower Cambrian Emu Bay Shale Konservat-Lagerstätte of South Australia. *J. Paleontol.* **92**, 80–86 (2018).
73. J. R. Paterson, J. B. Jago, G. A. Brock, J. G. Gehling, Taphonomy and palaeoecology of the emuellid trilobite *Balcoracania dailyi* (early Cambrian, South Australia). *Palaeogeogr. Paleoclimatol. Palaeoecol.* **249**, 302–321 (2007).
74. H. Yun, G. A. Brock, X. Zhang, L. Li, D. C. García-Bellido, J. R. Paterson, A new chancelloriid from the Emu Bay Shale (Cambrian Stage 4) of South Australia. *J. Syst. Palaeontol.* **17**, 1077–1087 (2019).
75. S. Clausen, X.-G. Hou, J. Bergström, C. Franzén, The absence of echinoderms from the Lower Cambrian Chengjiang fauna of China: Palaeoecological and palaeogeographical implications. *Palaeogeogr. Paleoclimatol. Palaeoecol.* **294**, 133–141 (2010).
76. F. Zhao, J.-B. Caron, D. J. Bottjer, S. Hu, Z. Yin, M. Zhu, Diversity and species abundance patterns of the early Cambrian (Series 2, Stage 3) Chengjiang Biota from China. *Paleobiology* **40**, 50–69 (2014).
77. K. Nanglu, J.-B. Caron, R. R. Gaines, The Burgess Shale paleocommunity with new insights from Marble Canyon, British Columbia. *Paleobiology* **46**, 58–81 (2020).
78. X. Yang, J. Kimmig, D. Zhai, Y. Liu, S. R. Kimmig, S. Peng, A juvenile-rich palaeocommunity of the lower Cambrian Chengjiang biota sheds light on palaeo-boom or palaeo-bust environments. *Nat. Ecol. Evol.* **5**, 1082–1090 (2021).
79. F. Chen, T. P. Topper, C. B. Skovsted, L. C. Strotz, J. Shen, Z. Zhang, Cambrian ecological complexities: Perspectives from the earliest brachiopod–supported benthic communities in the early Cambrian Guanshan Lagerstätte. *Gondwana Res.* **107**, 30–41 (2022).
80. D. C. García-Bellido, J. R. Paterson, G. D. Edgecombe, J. B. Jago, J. G. Gehling, M. S. Lee, The bivalved arthropods *Isoxys* and *Tuzoia* with soft-part preservation from the Lower Cambrian Emu Bay Shale Lagerstätte (Kangaroo Island, Australia). *Palaeontology* **52**, 1221–1241 (2009).
81. A. C. Daley, J. R. Paterson, G. D. Edgecombe, D. C. García-Bellido, J. B. Jago, New anatomical information on *Anomalocaris* from the Cambrian Emu Bay Shale of South Australia and a reassessment of its inferred predatory habits. *Palaeontology* **56**, 971–990 (2013).
82. J. R. Paterson, D. C. García-Bellido, G. D. Edgecombe, The early Cambrian Emu Bay Shale radiodonts revisited: Morphology and systematics. *J. Syst. Palaeontol.* **21**, 2225066 (2023).
83. F. Saleh, O. G. Bath-Enright, A. C. Daley, B. Lefebvre, B. Pittet, A. Vite, X. Ma, M. G. Mángano, L. A. Buatois, J. B. Antcliffe, A novel tool to untangle the ecology and fossil preservation knot in exceptionally preserved biotas. *Earth Planet. Sci. Lett.* **569**, 117061 (2021).
84. J. B. Jago, D. C. García-Bellido, J. G. Gehling, An early Cambrian chelicerate from the Emu Bay Shale, South Australia. *Palaeontology* **59**, 549–562 (2016).
85. R. D. Bicknell, J. D. Holmes, D. C. García-Bellido, J. R. Paterson, Malformed individuals of the trilobite *Estaingia bilobata* from the Cambrian Emu Bay Shale and their palaeobiological implications. *Geol. Mag.* **160**, 803–812 (2023).
86. D. C. García-Bellido, M. S. Lee, G. D. Edgecombe, J. B. Jago, J. G. Gehling, J. R. Paterson, A new vetulicolian from Australia and its bearing on the chordate affinities of an enigmatic Cambrian group. *BMC Evol. Biol.* **14**, 1–14 (2014).
87. R. R. Gaines, M. L. Droser, The paleoredox setting of Burgess Shale-type deposits. *Palaeogeogr. Palaeoclimatol. Palaeoecol.* **297**, 649–661 (2010).
88. D. M. Johnson, P. R. Hooper, R. M. Conrey, XRF analysis of rocks and minerals for major and trace elements on a single low dilution Li-tetraborate fused bead. *Adv. in X-ray Anal.* **41**, 843–867 (1999).
89. J. R. Paterson, J. B. Jago, J. G. Gehling, D. C. García-Bellido, G. D. Edgecombe, M. S. Lee, "Early Cambrian arthropods from the Emu Bay Shale Lagerstätte, South Australia" in *Advances in Trilobite Research* (Instituto Geológico y Minero de España, 2008), pp. 319–325.
90. J. B. Jago, B. J. Cooper, The Emu Bay Shale lagerstätte: A history of investigations. *Aust. J. Earth Sci.* **58**, 235–241 (2011).
91. J.-B. Caron, D. A. Jackson, Paleoecology of the greater phyllopod bed community, Burgess Shale. *Palaeogeogr. Palaeoclimatol. Palaeoecol.* **258**, 222–256 (2008).
92. S. Q. Dornbos, J.-Y. Chen, Community palaeoecology of the early Cambrian Maotianshan Shale biota: Ecological dominance of priapulid worms. *Palaeogeogr. Palaeoclimatol. Palaeoecol.* **258**, 200–212 (2008).
93. L. J. O'Brien, J.-B. Caron, Paleocommunity analysis of the Burgess Shale Tulip Beds, Mount Stephen, British Columbia: Comparison with the Walcott Quarry and implications for community variation in the Burgess Shale. *Paleobiology* **42**, 27–53 (2016).
94. G. D. Edgecombe, D. C. García-Bellido, J. R. Paterson, A new leanchoiliid megacheiran arthropod from the lower Cambrian Emu Bay Shale, South Australia. *Acta Palaeontol. Pol.* **56**, 385–400 (2011).
95. J. R. Paterson, G. D. Edgecombe, J. B. Jago, The 'great appendage' arthropod Tanglangia: Biogeographic connections between early Cambrian biotas of Australia and South China. *Gondwana Res.* **27**, 1667–1672 (2015).
96. J. R. Paterson, D. C. García-Bellido, G. D. Edgecombe, New artiopodan arthropods from the early Cambrian Emu Bay Shale Konservat-Lagerstätte of South Australia. *J. Paleontol.* **86**, 340–357 (2012).
97. J. R. Paterson, G. D. Edgecombe, D. C. García-Bellido, J. B. Jago, J. G. Gehling, Nektaspid arthropods from the lower Cambrian Emu Bay Shale Lagerstätte, South Australia, with a reassessment of lamellipedian relationships. *Palaeontology* **53**, 377–402 (2010).
98. G. D. Edgecombe, J. R. Paterson, D. C. Garcia-Bellido, A new aglaspidid-like euarthropod from the lower Cambrian Emu Bay Shale of South Australia. *Geol. Mag.* **154**, 87–95 (2017).
99. B. McHenry, A. Yates, First report of the enigmatic metazoan *Anomalocaris* from the Southern Hemisphere and a trilobite with preserved appendages from the Early Cambrian of Kangaroo Island, South Australia. *Rec. South Aust. Mus.* **26**, 77–86 (1993).
100. C. Nedin, The Emu Bay Shale, a Lower Cambrian fossil Lagerstätte. *Australas. Palaeontol. Mem.* **18**, 31–40 (1995).
101. K. J. Pocock, *Estaingia*, a new trilobite genus from the Lower Cambrian of South Australia. *Palaeontology* **7**, 458–471 (1964).
102. J. R. Paterson, G. D. Edgecombe, The Early Cambrian trilobite family Emuellidae Pocock, 1970: Systematic position and revision of Australian species. *J. Paleontol.* **80**, 496–513 (2006).
103. K. J. Pocock, The Emuellidae, a new family of trilobites from the Lower Cambrian of South Australia. *Palaeontology* **13**, 522–562 (1970).
104. J. R. Paterson, J. B. Jago, New trilobites from the Lower Cambrian Emu Bay Shale Lagerstatte at Big Gully, Kangaroo Island, South Australia. *Australas. Palaeontol. Mem.* **32**, 43 (2006).
105. S. Bengtson, *Early Cambrian Fossils from South Australia* (Association of Australasian Palaeontologists, 1990).
106. S. C. Morris, R. J. F. Jenkins, Healed injuries in early Cambrian trilobites from South Australia. *Alcheringa* **9**, 167–177 (1985).
107. R. D. Bicknell, J. D. Holmes, G. D. Edgecombe, S. R. Losso, J. Ortega-Hernández, S. Wroe, J. R. Paterson, Biomechanical analyses of Cambrian euarthropod limbs reveal their effectiveness in mastication and durophagy. *Proc. R. Soc. B* **288**, 20202075 (2021).
108. M. F. Glaessner, Lower Cambrian Crustacea and annelid worms from Kangaroo Island, South Australia. *Alcheringa* **3**, 21–31 (1979).
109. J. Dzik, Anatomy and relationships of the Early Cambrian *worm Myoscolex*. *Zool. Scr.* **33**, 57–69 (2004).
110. D. C. Garcia-Bellido, G. D. Edgecombe, J. R. Paterson, X. Ma, A 'Collins' monster'-type lobopodian from the Emu Bay Shale Konservat-Lagerstätte (Cambrian), South Australia. *Alcheringa* **37**, 474–478 (2013).

Acknowledgments: We thank the Buck family for access to localities; J. Chen, J. Creveling, and M. Prokopenko for beneficial discussions; numerous colleagues and volunteers who have helped with collection from the EBS quarry in the field; and J. Harris, W. Konwent, M. Lambert, M. Meyers, and C. Nellis for assistance in the laboratory. Artwork in Fig. 5 was produced by K. Kenny. **Funding:** This work was supported by the National Geographic Society [award 9332-16 (R.R.G.)], Australian Research Council [grants LP0774959 and FT120100770 (J.R.P.)] and FT130101329 (D.C.G.-B.), and National Science Foundation [award EAR-1849968 (P.M.M.)].
Author contributions: Conceptualization: R.R.G., D.G.C.-B., J.B.J., and J.R.P. Methodology: R.R.G., D.G.C.-B., J.B.J., P.M.M., and J.R.P. Investigation: R.R.G., D.G.C.-B., J.B.J., and J.R.P. Visualization: R.R.G., D.G.C.-B., and J.R.P. Writing—original draft: R.R.G., J.R.P., and P.M.M. Writing—review and editing: R.R.G., D.G.C.-B., J.B.J., P.M.M., and J.R.P. **Competing interests:** The authors declare that they have no competing interests. **Data and materials availability:** All data needed to evaluate the conclusions in the paper are present in the paper and/or the Supplementary Materials..

Submitted 15 March 2024
Accepted 25 June 2024
Published 26 July 2024
10.1126/sciadv.adp2650

Science Advances
AAAS

Supplementary Materials for

The Emu Bay Shale: A unique early Cambrian Lagerstätte from a tectonically active basin

Robert R. Gaines *et al.*

Corresponding author: Robert R. Gaines, robert.gaines@pomona.edu; John R. Paterson, jpater20@une.edu.au

Sci. Adv. **10**, eadp2650 (2024)
DOI: 10.1126/sciadv.adp2650

This PDF file includes:

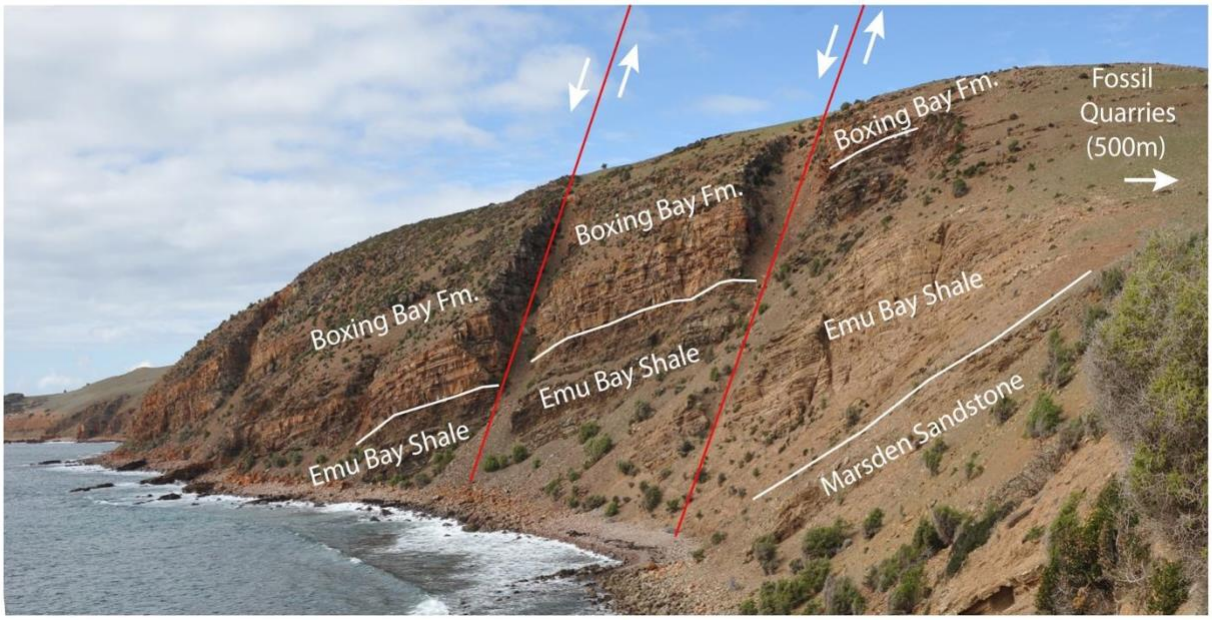

Fig. S1.

Exposure of Emu Bay Shale and adjoining units in sea cliffs along the shoreline immediately to the east of the mouth Big Gully on northeast coast of Kangaroo Island (Figure 1A, B). Red lines show the position of two normal faults (sense of motion shown by arrows) with displacements on the order of ~10 m. The mouth of Big Gully is at the right side of the image.

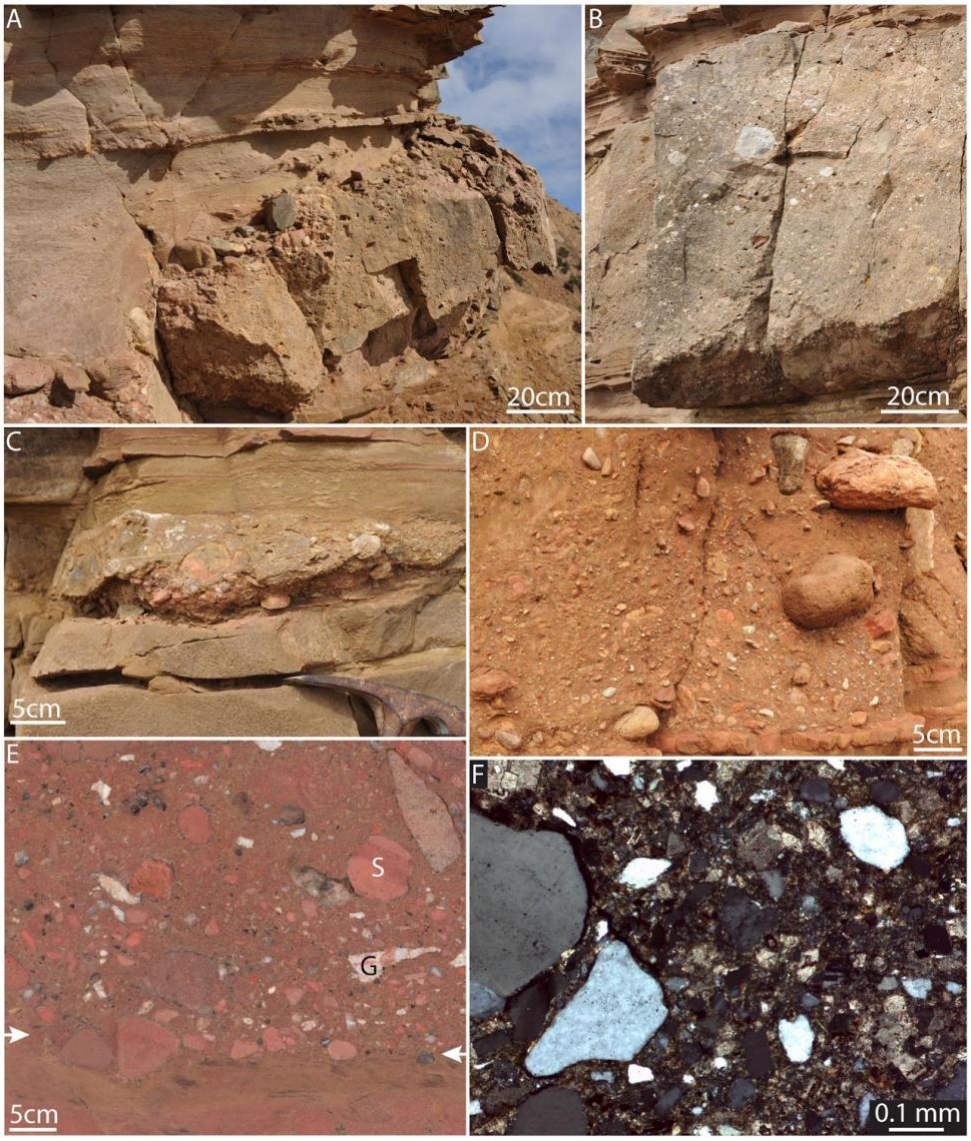

Fig. S2.

Conglomerates of the middle heterolithic unit of the EBS at the shoreline locality. A. Outcrop view of resistant paraconglomerate bed with sand matrix at 35.1 m. Accumulation of coarse gravel at bed top resulting from debris fall immediately following emplacement of paraconglomerate debris flow. B. Paraconglomerate including subrounded clasts, some in excess of 10 cm, at 32.5 m. C. Orthoconglomerate gravel lens at 31.9 m, which passes laterally into a horizon of isolated pebbles and cobbles residing in a mudstone matrix, shown in Fig. 2F. D. Paraconglomerate including large rounded-subrounded clasts at 32.5 m. E. Polished slab showing base of paraconglomerate at 32.1 m, including granitoid (G) and red siltstone (S) clasts. Contact (arrows) with underlying mudstone is non-erosive and deformed by loading of paraconglomerate into underlying mud. E. Polarized light micrograph of thin section of paraconglomerate, showing high matrix content and rounded-subrounded character of larger grains at 32.1 m.

Fig. S3.

Mudstones of the lower and middle EBS. A. Lowermost EBS mudstones in outcrop. B. large redlichiid trilobite, 3.7 m. C. Fossils of the soft bodied animal *Myoscolex* (M) and relatively small redlichiid trilobite (R) moult, 5.7 m. D. Transmitted light image of thin section of EBS mudstone showing faint lamination, hanging silt and very fine sand (bright spots) and clusters of oxidized pyrite (opaque), 7.95 m. F-G. Plane polarized light photomicrographs of EBS mudstones showing abundant micas (arrows) and a lens comprised of angular silt and very fine sand (G), 3.05 m and 2.95 m respectively.

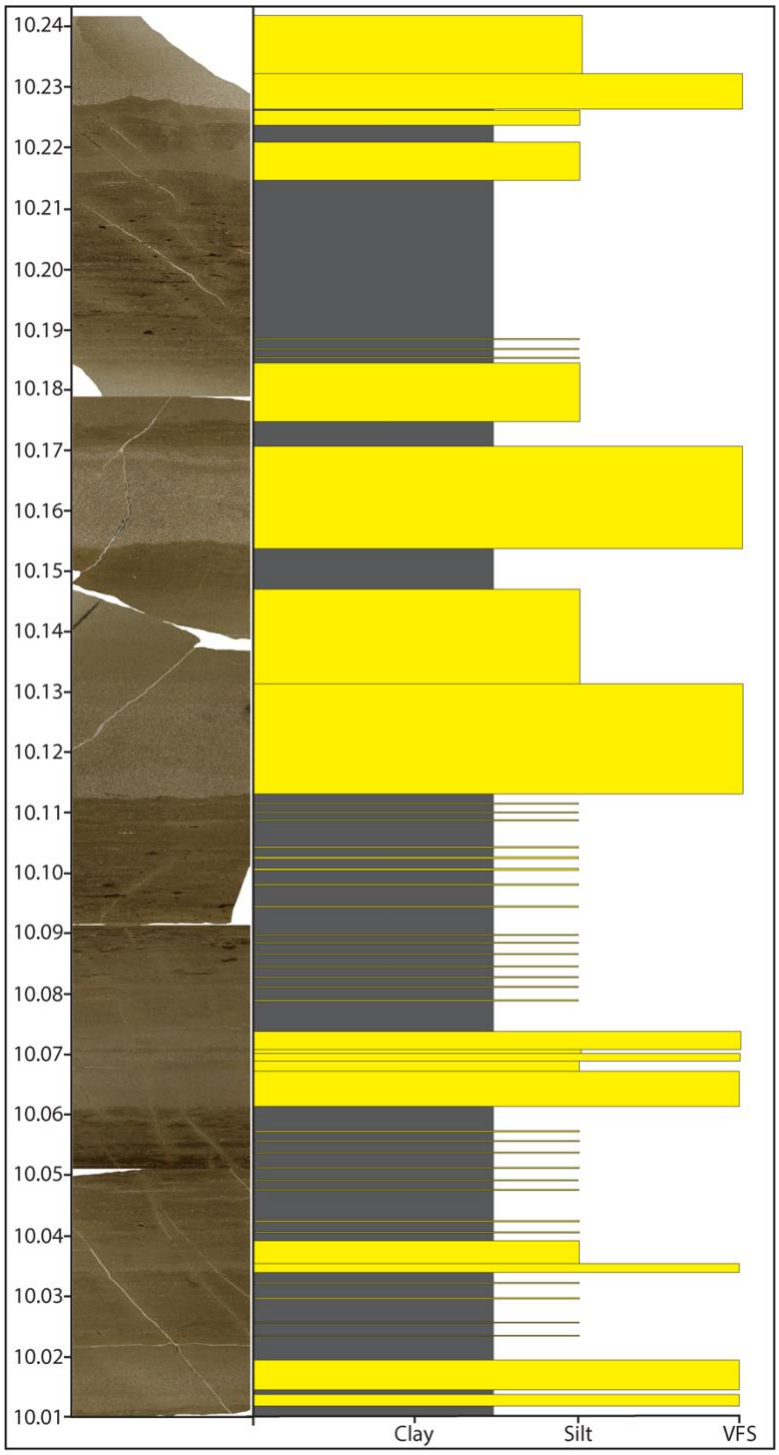

Fig. S4.
Detailed log of 23 cm interval within abundantly fossiliferous strata exposed in the lower mudstone unit at Buck Quarry (Fig. 1B, S1), with thin section images at left of log. Mudstones (dark) are characterized by faint lamination, hanging silt and very fine sand, and sub-mm "stringers" of very fine sand. Sands show high matrix content and lack of grading. Loading/dewatering structures commonly occur at mud/sand junctions, prominently at 10.23 m. Numbers on log indicate meters above base of the EBS.

Sample Depth	C [%]	S [%]
89.52	1.08	0.02
89.56	1.46	0.22
89.59	1.54	1.34
89.6	0.89	1.28
89.62	1.73	1.27
89.7	1.51	1.39
89.71	0.76	0.40
89.75	1.45	1.58
89.77	1.43	1.78
89.81	1.38	1.34
89.84	1.21	0.19
89.85	1.28	0.02
89.87	1.17	0.01
89.89	0.34	0.01
89.91	1.11	0.01
89.94	0.97	0.02
89.98	0.74	0.02
90.09	0.71	0.01
90.14	0.65	0.02
90.17	0.77	0.00
90.19	0.81	0.01
90.22	0.84	0.01
90.25	0.94	0.02
90.27	1.11	0.02
90.29	1.18	0.26
90.33	1.20	0.76
90.35	1.19	1.08
90.38	1.12	0.98
90.41	1.13	1.04
90.45	1.04	0.30
90.47	0.40	0.16
90.48	1.14	0.20
90.52	0.86	0.34
90.53	1.27	0.87
90.56	1.19	1.50
90.63	1.18	0.95
90.66	1.19	0.73
90.7	1.01	0.20
90.75	1.03	0.01
90.81	1.10	0.67
Average	1.08	0.53

Table S1.

Weight percent C and S determined for 40 borehole samples from the lower mudstone unit. Sample depth refers to position in core. As described in methods, sample powders were treated with 1M HCl to remove calcium carbonate and measured by combustion using an Elementar Vario Micro Cube.

Sample	Al2O3	Al	Mo	Mo/Al	EF--Mo
	(%)	(ppm)	(ppm)		
Average Shale (Wedepohl, 1977, 1991)				1.4623E-05	
BG1 80.35	13.61	72030.925	5	0.000069	4.75
BG1 80.65	15.53	82192.525	4	0.000049	3.33
BG1 81.70	14.34	75894.45	4	0.000053	3.60
BG1 82.00	14.1	74624.25	4	0.000054	3.67
BG1 82.18	13.1	69331.75	3	0.000043	2.96
BG1 82.50	14.13	74783.025	3	0.000040	2.74
BG1 83.05	13.13	69490.525	3	0.000043	2.95
BG1 83.20	13.79	72983.575	4	0.000055	3.75
BG1 83.40	13.16	69649.3	5	0.000072	4.91
BG1 84.00	13.82	73142.35	5	0.000068	4.67
BG1 84.10	13.76	72824.8	4	0.000055	3.76
BG1 84.20	13.43	71078.275	5	0.000070	4.81
BG1 84.40	12.63	66844.275	8	0.000120	8.18
BG1 84.50	14.32	75788.6	3	0.000040	2.71
BG1 84.70	13.31	70443.175	7	0.000099	6.80
BG1 84.90	12.85	68008.625	6	0.000088	6.03
BG1 85.05	12.65	66950.125	7	0.000105	7.15
BG1 85.30	12.7	67214.75	6	0.000089	6.10
BG1 85.60	14.25	75418.125	5	0.000066	4.53
BG1 85.87	13.57	71819.225	6	0.000084	5.71
BG1 86.10	14.42	76317.85	5	0.000066	4.48
BG1 86.30	14.31	75735.675	4	0.000053	3.61
BG1 86.45	13.08	69225.9	6	0.000087	5.93
BG1 87.20	14.57	77111.725	4	0.000052	3.55
BG1 87.35	14.66	77588.05	4	0.000052	3.53
BG1 87.50	14.28	75576.9	9	0.000119	8.14
BG1 87.70	14.99	79334.575	3	0.000038	2.59
BG1 87.90	13.66	72295.55	6	0.000083	5.68
BG1 88.08	14.58	77164.65	4	0.000052	3.54
BG1 86.60	13.95	73830.375	7	0.000095	6.48
BG1 88.80	11.45	60599.125	5	0.000083	5.64
BG1 88.90	12.41	65679.925	6	0.000091	6.25
BG1 89.10	13.36	70707.8	10	0.000141	9.67
BG1 83.20	13.77	72877.725	5	0.000069	4.69
BG1 89.52	12.8	67744	5	0.000074	5.05
BG1 89.56	13	68802.5	5	0.000073	4.97
BG1 89.59	12.38	65521.15	5	0.000076	5.22
BG1 89.60	10.24	54195.2	6	0.000111	7.57
BG1 89.64	12.19	64515.575	5	0.000078	5.30
BG1 89.67	12.51	66209.175	6	0.000091	6.20
BG1 89.70	12.48	66050.4	5	0.000076	5.18
BG1 89.71	11.13	58905.525	6	0.000102	6.97
BG1 89.75	12.63	66844.275	6	0.000090	6.14
BG1 89.77	12.9	68273.25	6	0.000088	6.01
BG1 89.79	12.74	67426.45	5	0.000074	5.07
BG1 89.81	12.68	67108.9	5	0.000075	5.10
BG1 89.84	12.61	66738.425	6	0.000090	6.15
BG1 89.85	12.88	68167.4	6	0.000088	6.02
BG1 89.87	12.54	66367.95	5	0.000075	5.15
BG1 89.89	7.77	41122.725	5	0.000122	8.31
BG1 89.91	12.62	66791.35	5	0.000075	5.12
BG1 89.94	12.06	63827.55	5	0.000078	5.36
BG1 89.98	12.18	64462.65	5	0.000078	5.30
BG1 90.09	13.03	68961.275	5	0.000073	4.96
BG1 90.14	12.79	67691.075	6	0.000089	6.06
BG1 90.17	12.93	68432.025	5	0.000073	5.00
BG1 90.19	12.73	67373.525	5	0.000074	5.08
BG1 90.22	12.45	65891.625	6	0.000091	6.23
BG1 90.25	12.22	64674.35	5	0.000077	5.29
BG1 90.27	12.39	65574.075	6	0.000091	6.26
BG1 90.29	12.51	66209.175	4	0.000060	4.13
BG1 90.31	12.18	64462.65	5	0.000078	5.30
BG1 90.33	12.73	67373.525	4	0.000059	4.06
BG1 90.35	12.41	65679.925	5	0.000076	5.21
BG1 90.38	12.64	66897.2	4	0.000060	4.09
BG1 90.41	12.12	64145.1	5	0.000078	5.33
BG1 90.45	12.22	64674.35	4	0.000062	4.23
BG1 90.47	9.76	51654.8	5	0.000097	6.62
BG1 90.48	12.46	65944.55	5	0.000076	5.19
BG1 90.52	12.42	65732.85	5	0.000076	5.20
BG1 90.53	13.39	70866.575	4	0.000056	3.86
BG1 90.55	12.86	68061.55	5	0.000073	5.02
BG1 90.58	12.67	67055.975	4	0.000060	4.08
BG1 90.61	12.34	65309.45	5	0.000077	5.24
BG1 90.63	12.72	67320.6	4	0.000059	4.06
BG1 90.66	12.57	66526.725	5	0.000075	5.14
BG1 90.70	12.31	65150.675	5	0.000077	5.25
BG1 90.75	13.28	70284.4	4	0.000057	3.89
BG1 90.80	13.47	71289.975	7	0.000098	6.71
BG1 91.00	14.07	74465.475	6	0.000081	5.51
BG1 91.20	13.02	68908.35	6	0.000087	5.95
BG1 91.40	12.45	65891.625	6	0.000091	6.23
BG1 91.60	13.6	71978	5	0.000069	4.75
BG1 91.75	13.49	71395.825	4	0.000056	3.83
BG1 91.90	13.97	73936.225	4	0.000054	3.70
BG1 92.10	13.73	72666.025	4	0.000055	3.76
BG1 92.30	14.65	77535.125	4	0.000052	3.53
BG1 93.50	17.31	91613.175	11	0.000120	8.21
BG1 93.60	16.84	89125.7	12	0.000135	9.21
BG1 93.70	15.59	82510.075	14	0.000170	11.60
BG1 93.85	16.28	86161.9	11	0.000128	8.73
BG1 94.10	15.81	83674.425	8	0.000096	6.54
BG1 94.20	16.91	89496.175	3	0.000034	2.29
AVERAGE	**13.2186022**	**69959.4519**	**5.39784946**	**0.000077**	**5.29**

Table S2.

Concentrations of Al and Mo as measured from XRF for 93 borehole samples from the *Konservat-Lagerstätte* interval, with Enrichment Factor for Mo (EF-Mo) calculated using average shale value (shown at top; from Wedepohl 1977, 1991) as described in methods.

Table S3. Emu Bay Shale faunal data from the Konservat-Lagerstätte interval at Big Gully.

Specimen counts are based on the number of registered Emu Bay Shale Konservat-Lagerstätte specimens in the South Australian Museum (SAM; Adelaide) palaeontology collection as of December 2017 (*ca.* 5800 specimens), in addition to observations of associated (unregistered) individuals on the same pieces of rock. This includes material sourced from Buck and Daily quarries, in addition to the shoreline locality. Life mode includes information on tiering and mobility only—following similar categories used in previous studies (*76, 77, 91–93*)—as feeding habits (e.g., suspension/filtering, deposit, hunting/scavenging, grazing) are largely unknown for many Emu Bay Shale species.

General abundance categories and abbreviations: VR (very rare: <10 specimens); R (rare: 10–100 specimens); C (common: 101–500 specimens); A (abundant: 501–1000); VA (very abundant: >1000).

Taxa	Approx. number of specimens	General abundance	Probable life mode [M – Mobile; S – Sessile]	Endemic to EBS at genus level	Key references
ANNELIDA					
Polychaeta					
Burgessochaetidae? gen. et sp. indet.	1	VR	Epibenthic [M]	?	(*14*)
ARTHROPODA					
Megacheira/'chelicerate-like forms'					
Oestokerkus megacholix	128	C	Nektonic or nektobenthic [M]	Yes	(*94*)
Tanglangia rangatanga	42	R	Nektonic or nektobenthic [M]	No	(*95*)
Wisangocaris barbarahardyae	462	C	Nektobenthic [M]	Yes	(*84, 85*)
Non-trilobite artiopodans					
'Xiphosuran-like' artiopodan	2	VR	Epibenthic [M]	Yes	Not applicable
Australimicola spriggi	24	R	Epibenthic [M]	Yes	(*96*)
"Chevron Guy"	9	VR	Epibenthic [M]	Yes	Not applicable
Emucaris fava	46	R	Epibenthic [M]	Yes	(*97*)
Eozetetes gemmelli	2	VR	Epibenthic [M]	Yes	(*98*)
Kangacaris zhangi	27	R	Epibenthic [M]	No	(*97*)
Squamacula buckorum	68	R	Epibenthic [M]	No	(*96*)
Xandarellida gen. et sp. nov.	3	VR	Epibenthic [M]	Yes	Not applicable
Radiodonta					
Echidnacaris briggsi	156[a]	C	Nektonic [M]	Yes	(*5, 7, 81, 82, 99, 100*)
Anomalocaris daleyae	*ca.* 20[a]	R	Nektonic [M]	No	(*6, 7, 81, 82, 100*)
Trilobita					
Balcoracania dailyi	6	VR	Epibenthic [M]	No	(*102, 103*)
Estaingia bilobata	20,880[b]	VA	Epibenthic [M]	No	(*62–64, 68, 85, 100, 101*)
Holyoakia simpsoni	9	VR	Epibenthic [M]	No	(*104*)
Megapharanaspis nedini	13	R	Epibenthic [M]	Yes	(*104*)

Redlichia takooensis	522	A	Epibenthic [M]	No	(*62, 65, 66, 104, 105*)
Redlichia rex	*ca.* 50	R	Epibenthic [M]	No	(*65, 66, 85, 99, 104, 106, 107*)
Uncertain					
Arthropod with large setose exopods	2	VR	Nektonic or nektobenthic [M]	?	Not applicable
Canadaspidida gen. et sp. indet.	34	R	Nektonic or nektobenthic [M]	?	Not applicable
"Football Guy"	171	C	Nektonic or nektobenthic [M]	Yes	Not applicable
Isoxys communis	*ca.* 550	A	Nektonic [M]	No	(*80, 108*)
Isoxys glaessneri	43	R	Nektonic [M]	No	(*80*)
Mollisoniidae gen. et sp. indet.	23	R	Epibenthic [M]	?	Not applicable
Myoscolex ateles	393	C	Nektonic or nektobenthic [M]	Yes	(*4, 108, 109*)
Parapaleomerus? sp.	2	VR	Epibenthic [M]	?	Not applicable
Tuzoia australis	204	C	Nektonic [M]	No	(*80, 108*)
Tuzoia sp. nov.	*ca.* 10	R	Nektonic [M]	No	(*80*)
"Zipper Guy"	48	R	Epibenthic [M]	Yes	Not applicable
BRACHIOPODA					
Diandongia sp.	19[c]	R	Epibenthic [S]	No	(*14*)
Eoobolidae gen. et sp. indet.	4[c]	VR	Epibenthic [S]	?	(*14*)
CHORDATA					
Vetulicolia					
Nesonektris aldridgei	301	C	Nektonic [M]	Yes	(*86*)
ONYCHOPHORA					
Luolishaniidae gen. et sp. indet.	1	VR	Epibenthic [M]	?	(*110*)
PORIFERA					
Choiidae gen. et sp. indet.	1	VR	Epibenthic [S]	?	(*14*)
Hamptoniidae gen. et sp. indet.	3	VR	Epibenthic [S]	?	(*14*)
Leptomitidae gen. et sp. indet.	130[d]	C	Epibenthic [S]	?	(*14*)
PRIAPULIDA					
Palaeoscolecida					
Wronascolex antiquus	*ca.* 350	C	Endobenthic [M]	No	(*69, 108*)
Wronascolex iacoborum	1	VR	Endobenthic [M]	No	(*69*)
Uncertain					
Priapulida gen. et sp. indet.	3	VR	Endobenthic [M]	?	Not applicable
UNCERTAIN / OTHER					
Chancelloriida					
Chancelloria australilonga	3	VR	Epibenthic [S]	No	(*74*)
Eldonioidea					
Rotadiscidae gen. et sp. indet.	2	VR	Unknown	?	(*72*)

Hyolitha					
Hyolitha gen. et sp. indet. A (ribbed)	20[e]	R	Epibenthic [S]	?	(*14*)
Hyolitha gen. et sp. indet. B (smooth)	6[e]	VR	Epibenthic [S]	?	(*14*)
Nectocarididae					
Vetustovermis planus	34	R	Nektonic [M]	No	(*14, 108*)
Other					
"Petalloid"	522	A	Epibenthic [S]	Yes	(*14*)
Scleritome animal	3	VR	Epibenthic [M]	Yes	Not applicable
"Stingray Guy"	2	VR	Unknown	Yes	Not applicable
Taxon w/series of mesh-like lobe structures	4	VR	Unknown	Yes	Not applicable

[a] Number represents single frontal appendages only. Thus, number of individuals of each radiodont species represents half of this total.

[b] Based on preliminary census data, there is an average of 3.6 individuals associated with each registered specimen of any species on the same piece of rock. Thus, it is estimated that the SAM collection contains >20,000 individuals of *Estaingia bilobata*.

[c] Number represents single valves only. Thus, number of individuals represents half of this total.

[d] Specimens may represent more than one species.

[e] Number represents conchs only. Opercula are extremely rare and helens have not been observed.